Chinese Medical Journal®

Effects of *COL1A1* and *SYTL2* on inflammatory cell infiltration and poor extracellular matrix remodeling of the vascular wall in thoracic aortic aneurysm

Xinsheng Xie[1], Ye Yuan[2,3], Yulong Huang[1], Xiang Hong[1], Shichai Hong[1], Gang Chen[1], Yihui Chen[1], Yue Lin[1], Weifeng Lu[1], Weiguo Fu[1,2,3], Lixin Wang[1,2,3]

[1]Department of Vascular Surgery, Zhongshan Hospital (Xiamen), Fudan University, Xiamen,Fujian 361015, China;
[2]Department of Vascular Surgery, Zhongshan Hospital, Fudan University, Shanghai 200032, China;
[3]Vascular Surgery Institute of Fudan University, Fudan University, Shanghai 200032, China.

Abstract

Background: Thoracic aortic aneurysm (TAA) is a fatal cardiovascular disease, the pathogenesis of which has not yet been clarified. This study aimed to identify and validate the diagnostic markers of TAA to provide a strong theoretical basis for developing new methods to prevent and treat this disease.

Methods: Gene expression profiles of the GSE9106, GSE26155, and GSE155468 datasets were acquired from the Gene Expression Omnibus (GEO) database. Differentially expressed genes (DEGs) were identified using the "limma" package in R. Least absolute shrinkage and selection operator (LASSO), support vector machine-recursive feature elimination (SVM-RFE), random forest, and binary logistic regression analyses were used to screen the diagnostic marker genes. Single-sample gene set enrichment analysis (ssGSEA) was used to estimate immune cell infiltration in TAA.

Results: A total of 16 DEGs were identified. The enrichment and functional correlation analyses showed that DEGs were mainly associated with inflammatory response pathways and collagen-related diseases. Collagen type I alpha 1 chain (*COL1A1*) and synaptotagmin like 2 (*SYTL2*) were identified as diagnostic marker genes with a high diagnostic value for TAA. The expression of *COL1A1* and *SYTL2* was considerably higher in TAA vascular wall tissues than in the corresponding normal tissues, and there were significant differences in the infiltration of immune cells between TAA and normal vascular wall tissues. Additionally, *COL1A1* and *SYTL2* expression were associated with the infiltration of immune cells in the vascular wall tissue. Single-cell analysis showed that *COL1A1* in TAA was mainly derived from fibroblasts and *SYTL2* mainly from cluster of differentiation (CD)8^+ T cells. In addition, single-cell analysis indicated that fibroblasts and $CD8^+$ T cells in TAA were significantly higher than those in normal arterial wall tissue.

Conclusions: *COL1A1* and *SYTL2* may serve as diagnostic marker genes for TAA. The upregulation of *SYTL2* and *COL1A1* may be involved in the inflammatory infiltration of the vessel wall and poor extracellular matrix remodeling, promoting the progression of TAA.

Keywords: Bioinformatics; Thoracic aortic aneurysm; Immune response; Single cell analysis; *COL1A1*; *SYTL2*; Machine learning

Introduction

Thoracic aortic aneurysm (TAA) refers to the pathological expansion of the thoracic aorta that exceeds 50% of the normal diameter or the diameter is >5 cm. It is an extremely dangerous macrovascular disease with a high mortality rate.[1,2] TAAs are caused by a variety of complex factors, including genetics and environment. Joyce *et al*[3] found in 1964 that about 50% of patients with TAAs died within five years of diagnosis. The 5-year survival rate for symptomatic aneurysms and asymptomatic aneurysms is about 26.9% and 58.3%, respectively. Recently, a study of UK administrative data showed that freedom from mortality at 5 years was only 65% after thoracic endovascular aortic repair (TEVAR), compared with 89% in matched controls, which suggests that this group has a generally poorer life expectancy than that of the normal population.[4,5] At present, some progress has been made in the research of TAA in genetics, proteomics, hemodynamics, and treatment methods; however, there is still a high mortality rate, and there is no clinically feasible method to prevent the

Access this article online

Quick Response Code:

Website: www.cmj.org

DOI: 10.1097/CM9.0000000000002808

Correspondence to: Lixin Wang, Department of Vascular Surgery, Zhongshan Hospital (Xiamen), Fudan University, Xiamen, Fujian 361015, China; Department of Vascular Surgery, Zhongshan Hospital, Fudan University, Shanghai 200032, China; Vascular Surgery Institute of Fudan University, Fudan University, Shanghai 200032, China
E-Mail: wang.lixin@ zs-hospital.sh.cn

Chinese Medical Journal 2024;137(9)
Received: 15-02-2023; **Online:** 28-08-2023 **Edited by:** Ting Gao and Xiuyuan Hao

occurrence of aortic aneurysm.[6,7] Therefore, early diagnosis and identification of TAAs are important.

Current studies have shown that the pathogenesis of TAA may involve genetic factors, intra-arterial hemodynamic changes, vascular wall inflammation, and extracellular matrix remodeling.[8] The thoracic aorta wall consists of three components: Elastic fibers, smooth muscle cells (SMCs), and collagen. It is the basic unit of the structure and function of the thoracic aortic wall and determines its mechanical properties. Both elastin and collagen are load-carrying proteins at high pressures and marked caliber expansion. The ratio of collagen to elastin basically determines the mechanical properties of the vessel wall.[1] Inflammatory cell infiltration and elevated levels of inflammatory cytokines have been found in aortic tissue in patients with TAA or mouse models, suggesting that inflammation may play an important role in the development of the disease. There is inflammatory infiltration in the wall of TAA, especially in the middle layer of the ruptured aneurysm wall, and a large number of inflammatory cells accumulate.[9,10] The expression of inflammation-related genes, such as chemokines, tumor necrosis factor (TNF), toll-like receptor-2, and cluster of differentiation 14 (CD14) antigen genes, are all upregulated in local aneurysm tissue.[11] In the pathophysiological process of many cardiovascular diseases, the expression and activity of matrix metalloproteinases (MMPs) are enhanced, and the mobilization and activation of inflammatory cells aggravate the inflammatory response of the aneurysm wall tissue and the structural disorder of the extracellular matrix, such as elastic fibers and collagen fibers, which in turn promotes the remodeling and swelling of the blood vessel wall.[12]

In recent years, technologies such as ribonucleic acid (RNA) sequencing and gene chips have continued to develop. While accuracy and efficiency have increased, technical costs have also decreased, leading to large disease-related databases.[13] Using bioinformatics to mine these databases, we can easily find genes that may be related to the occurrence and development of TAA. Compared to traditional research, it is more economical and effectively shortens the research cycle. Our study used bioinformatics and statistical methods to identify and validate the diagnostic markers of TAA, which maybe provide the theoretical basis for the development of a new molecular mechanism study in TAA.

Methods

Ethical approval

All procedures performed in studies involving human participants were in accordance with the ethical standards of the institutional research committee and with the 1964 *Helsinki Declaration* and its later amendments or comparable ethical standards. This study was approved by the Ethics Committee of Zhongshan Hospital, Fudan University (No. B2021-718R). Written informed consent was obtained from the patient before surgery.

Data processing and differentially expressed gene (DEG) screening

Datasets (GSE9106, GSE26155, and GSE155468) from the Gene Expression Omnibus (GEO) database (https://www.ncbi.nlm.nih.gov/geo/) were selected. The GSE9106 dataset contained peripheral blood cell data from 59 TAAs and 34 normal aortic samples. The GSE26155 dataset contained 43 TAAs and 43 normal aortic sample data from the aortic wall tissues. The GSE155468 dataset contains single-cell transcriptome data from one TAA and one normal aortic sample from aortic wall tissues. The "sva" package from R language software, version 4.1.1 (https://www.r-project.org/) was used to normalize datasets and the "limma" R package to identify differentially expressed genes (DEGs). Considering the difference between peripheral blood samples and aortic wall tissue samples, an adjusted P value <0.05 and $|\log_2$ fold change (FC)$|$ >0.5 were considered statistically significant.

Enrichment and functional analysis of DEGs

Gene Ontology (GO: included biological process, molecular function, and cellular component), Kyoto Encyclopedia of Genes and Genomes (KEGG), Disease Ontology (DO), and gene set enrichment analysis (GSEA) were performed for DEGs with "ClusterProfiler" R package and the gene sets "c5. go. v7.4. symbols. gmt (https://www.gsea-msigdb.org/gsea/login.jsp)", and "c2.cp.kegg. v7.0.symbols.gmt (https://www.gsea-msigdb.org/gsea/index.jsp)". Statistical significance was set at P <0.05.

Immune analysis

Single-sample GSEA (ssGSEA) was used to analyze the scores for infiltrating immune cells and immune functions. Correlation heatmaps and plotting correlative data ("corrplot" package) were used to show the relationship between infiltrating immune cells and immune function.

Single-cell analysis

In total, 1836 cells from aortic wall tissues (one TAA and one normal aortic sample) were included in this analysis. The "Seurat" package was used for quality control, statistical analysis, and exploration of the data. The t-distributed stochastic neighbor embedding algorithm was applied for dimensionality reduction with initial principal components (PCs) and cluster classification analysis across all cells. The "limma" package in R was used to identify the marker genes of each cluster with an adjusted P-value <0.05 and $|\log_2$ [FC]$|$ >0.5. The "SingleR" package was used to determine and annotate different cell clusters.

Immunofluorescence staining

For immunofluorescence, sections were prepared in the same manner as for immunohistochemistry (IHC), until primary antibody incubation. Subsequently, after overnight incubation with an anti-Collagen I antibody (1:200; mouse. No. ab138492; Abcam; Shanghai, China), anti-CD163 antibody (1:300; rabbit. No. ab138492;

Abcam), and anti-SYTL2 antibody (1: 250; rabbit. No. ab251097; Abcam) in a humidified chamber at 4℃ , phosphate buffered saline (PBS) washing was performed three times, and fluorescein-labeled secondary antibodies (sheep anti-rabbit IgG H&L, fluorescein isothiocyanate [FITC]; 1:1000, rabbit. No. ab6791; Abcam) and (Goat Anti-Mouse IgG H&L [Alexa Fluor® 488]; 1: 1000, No. ab150117; Abcam) were added and incubated at room temperature for 1 h in the dark. PBS was used to wash sections in the dark three times. 4′-6-diamidino-2-phenylindole (DAPI) staining solution was then added drop-wise, and coverslips were mounted onto a glass slide (Santa Cruz Biotechnology, Inc., Dallas, TX, USA), which was incubated at room temperature for 1 min in the dark. Images were captured with a confocal microscope (IX-70; Olympus Corporation; Tokyo, Japan).

Verhoeff's van gieson (EVG) staining

The tissue was fixed with formaldehyde solution, sliced in paraffin, and conventionally dewaxed to water. Wash with 70% ethanol and dip 15 mL of Victoria Blue B solution. Differentiation in 95% ethanol for a few seconds. Wash twice in distilled water. Dye with Ponceau drops for 5 min. Differentiation and dehydration with anhydrous ethanol. Soak slides with xylene to make them transparent and seal with a neutral adhesive. Microscope observation.

Statistical analysis

Data were statistically analyzed using R language software, https://www.r-project.org/. Differences were considered statistically significant at a P value <0.05. The results were expressed as percentages or mean ± standard deviation (SD) unless otherwise noted. Data were analyzed using the chi-squared test, Fisher's exact test, or Student's t-test. To screen for biomarker genes in TAA, the support vector machine-recursive feature elimination (SVM-RFE) "e1071" packages algorithm, random forest algorithm ("randomForest" package), least absolute shrinkage and selection operator (LASSO) algorithm ("glmnet" package), and binary logistic regression were performed. The prediction efficiency of biomarker genes for TAA was tested using a neural network model, nomogram, cluster analysis, and receiver operating characteristic curves.

Results

DEG screening

In the GSE9106 dataset, we analyzed 59 TAA and 34 normal samples of peripheral blood cells, and 21 DEGs were identified using the "limma" package between the two groups. In the GSE26155 dataset, we analyzed 43 TAA and 43 normal samples of the aortic wall tissues, and 21 DEGs were identified by using the "limma" package between the two groups. The cut-off values were adjusted to P value <0.05 and |log FC| >0.5. The flowchart of this study was shown in Supplementary Figure 1A, http://links.lww.com/CM9/B669. Heatmaps and volcano plots of the DEGs in the two datasets were shown in Supplementary Figure 1B–E, http://links.lww.com/CM9/B669.

Enrichment and functional correlation analysis of DEGs

Venn diagram identified the 16 common DEGs (coDEGs) of GSE9106 and GSE26155 from the peripheral blood and the arterial wall tissue, respectively [Figure 1A]. GO analysis of DEGs showed that the top three terms in biological processes included positive regulation of T cell differentiation in the thymus, regulation of phosphatidylinositol 3-kinase signaling, and regulation of T cell differentiation in the thymus. The cellular component groups included collagen trimers and the external side of the plasma membrane. In molecular functions, TAA was mainly enriched on cargo receptor activity, modified amino acid binding, and amide binding [Figure 1B]. KEGG pathway analysis revealed that the DEGs were mainly involved in the phosphatidylinositol 3-kinase-Akt kinase (PI3K-AKT) signaling pathway [Figure 1C]. Diseases enriched by DEGs mainly included Ehlers–Danlos syndrome [Figure 1D]. The GSEA results showed that the enriched pathways mainly involved chemokine signaling pathway, complement and coagulation cascades, and cytokine–cytokine receptor interaction in TAA, but butanoate metabolism, cardiac muscle contraction, and oxidative phosphorylation in control group [Figure 1E, F]. These results suggested that inflammatory responses and collagen-related diseases played important roles in TAA pathogenesis.

Biomarker gene screening and diagnosability test

To screen diagnostic marker genes, the SVM-RFE algorithm, random forest algorithm, LASSO algorithm, and binary logistic regression were performed. The binary logistic regression algorithm was used to identify four DEGs as diagnostic markers for TAA [Figure 2A]. Three genes were identified from the DEGs by using the Random forest algorithm as diagnostic markers [Figure 2B, C]. Sixteen genes were identified from the DEGs by using the SVM-RFE algorithm as diagnostic markers [Figure 2D]. The LASSO logistic regression algorithm was used to identify four DEGs as diagnostic markers for TAA [Figure 2E, F]. Collagen type I alpha 1 chain (*COL1A1*) and synaptotagmin like 2 (*SYTL2*) were finally obtained from the overlap of the random forest, LASSO, SVM-RFE, and binary logistic regression analyses [Figure 2G].

COL1A1 and *SYTL2* expression was considerably higher in the TAA vascular wall than in the corresponding normal tissues, and the expression of *COL1A1* was positively correlated with *SYTL2* [Figure 3A, B]. Nomogram maps were constructed to predict the probability of TAA using *COL1A1* and *SYTL2* [Figure 3C]. The calibration plots indicated that the nomogram performed well in predicting the rupture probability in patients with TAA [Figure 3D, E]. The area under curve (AUC, 0.95; 95% confidence interval [CI]: 0.93–0.97) indicated that *COL1A1* and *SYTL2* (in the nomogram model) had an accurate predictive value for TAA [Figure 3F]. The cali-

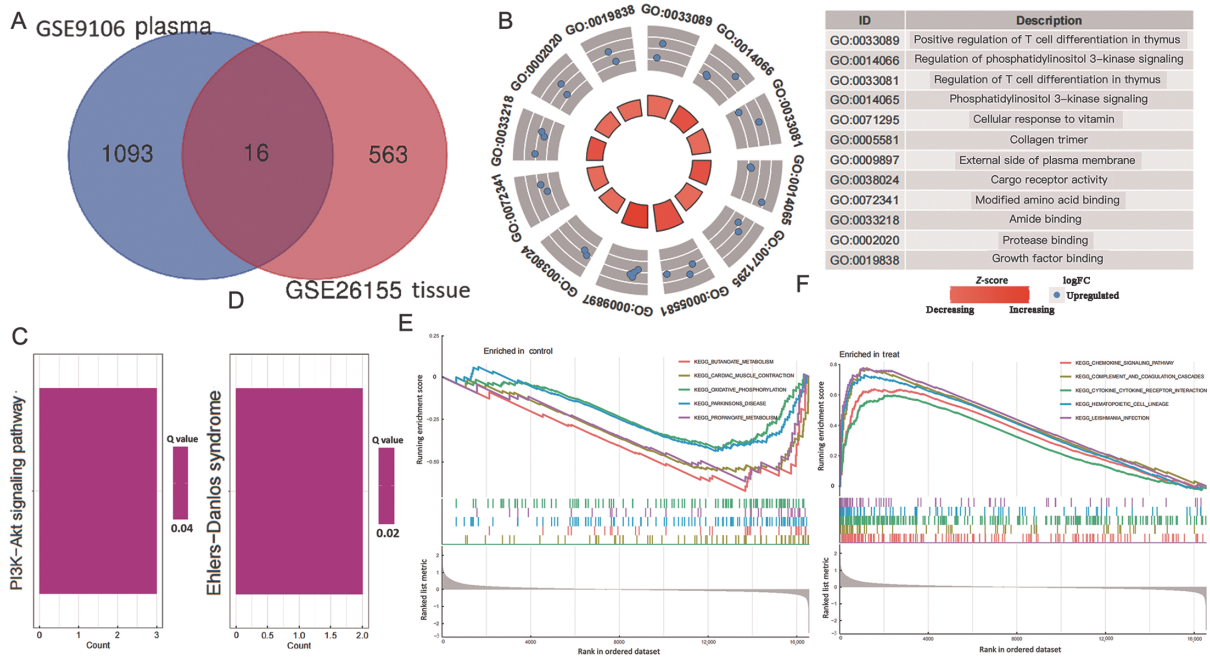

Figure 1: Enrichment and functional correlation analysis of the DEGs of GSE9106 dataset and GSE26155 dataset. (A) Venn diagram identified the 16 common DEGs. (B) GO enrichment analyses of DEGs. The farther the dot was from the center of the circle, the more up-regulated the GO term was. (C) KEGG enrichment analyses of DEGs. (D) DO enrichment analysis of the DEGs by histogram plot. (E) GSEA analysis of the KEGG pathway terms for DEGs enriched in the normal group. (F) GSEA analysis of the KEGG pathway terms for DEGs enriched in the TAA group. DEGs: Differentially expressed genes; DO: Disease Ontology; GO: Gene Ontology; GSEA: Gene set enrichment analysis; KEGG: Kyoto Encyclopedia of Genes and Genomes; TAA: Thoracic aortic aneurysm. Biomarker gene screening and diagnosability test

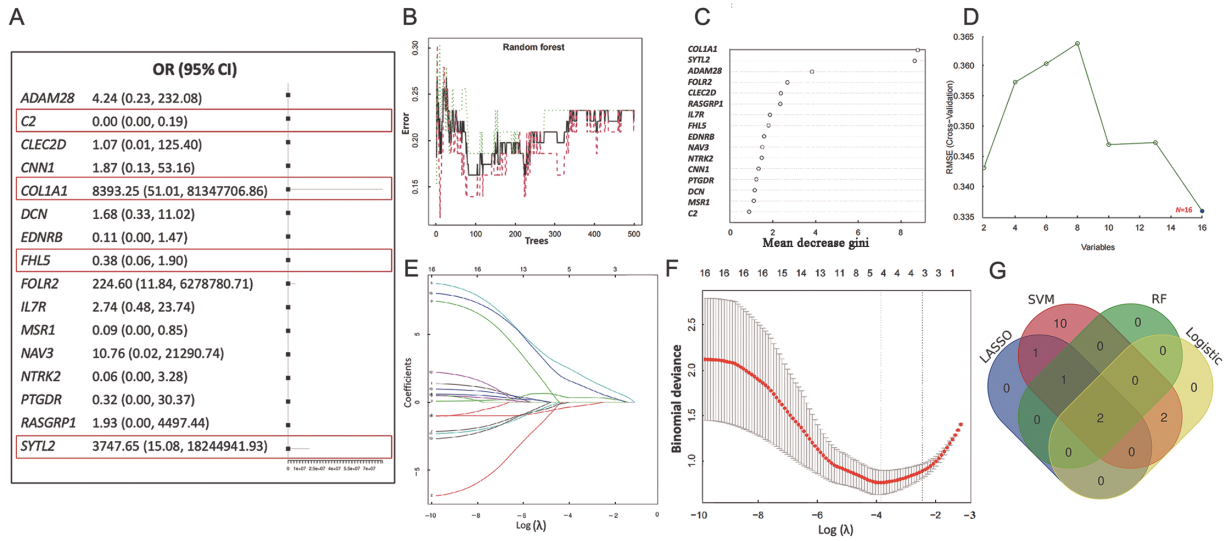

Figure 2: Screen the hub genes by the four methods of analysis. (A) Binary logistic regression identification of key genes of the DEGs. The binary logistic regression algorithm was used to identify four DEGs (*C2, COL1A1, FHL5, SYTL2*) as diagnostic markers for TAA. (B) The random forest tree for the identification of key genes of the DEGs. (C) The importance of the variables based on the RF model. (D) A plot of biomarkers selection via SVM-RFE algorithm. (E) LASSO logistic regression identification of hub genes of the DEGs. (F) Identification of optimal λ value based on cross-validation. (G) Venn diagram identified the key genes integrated the all identified methods above. DEGs: Differentially expressed genes; LASSO: Least absolute shrinkage and selection operator. TAA: Thoracic aortic aneurysm; SVM-RFE: Support vector machine-recursive feature elimination. RF: Random forest. ADAM28: A disintegrin and metallopeptidase domain 28; C2: Complement C2; CLEC2D: C-type lectin domain family 2 member D; CNN1: Calponin 1; COL1A1: Collagen type I alpha 1 chain; DCN: Decorin; EDNRB: Endothelin receptor type B; FHL5: Four and a half LIM domains 5; FOLR2: Folate receptor beta; IL7R: Interleukin 7 receptor; MSR1: Macrophage scavenger receptor 1; NAV3: Neuron navigator 3; NTRK2: Neurotrophic receptor tyrosine kinase 2; PTGDR: Prostaglandin D2 receptor; RASGRP1: RAS guanyl releasing protein 1; SYTL2: Synaptotagmin like 2. EMSE: Emseble Learning.

bration plots indicated that the nomogram performed well in predicting rupture probability in patients with TAA. We then constructed an artificial neural network model using *COL1A1* and *SYTL2* [Figure 3G]. The AUC (AUC = 0.88, 95% CI: 0.81–0.94 in GSE26155 and AUC = 0.67, 95% CI: 0.55–0.77 in GSE9106) indi-

cated that *COL1A1* and *SYTL2* (in the artificial neural network model) produced an accurate predictive value for TAA [Figure 3H, I]. In addition, according to the expression levels of *COL1A1* and *SYTL2*, we performed cluster analysis on GSE26155 and GSE9106. The clustering results showed that *COL1A1* and *SYTL2* clearly divided the two datasets into two parts [Figure 3J,L]. We performed a chi-squared test on the clustering results,

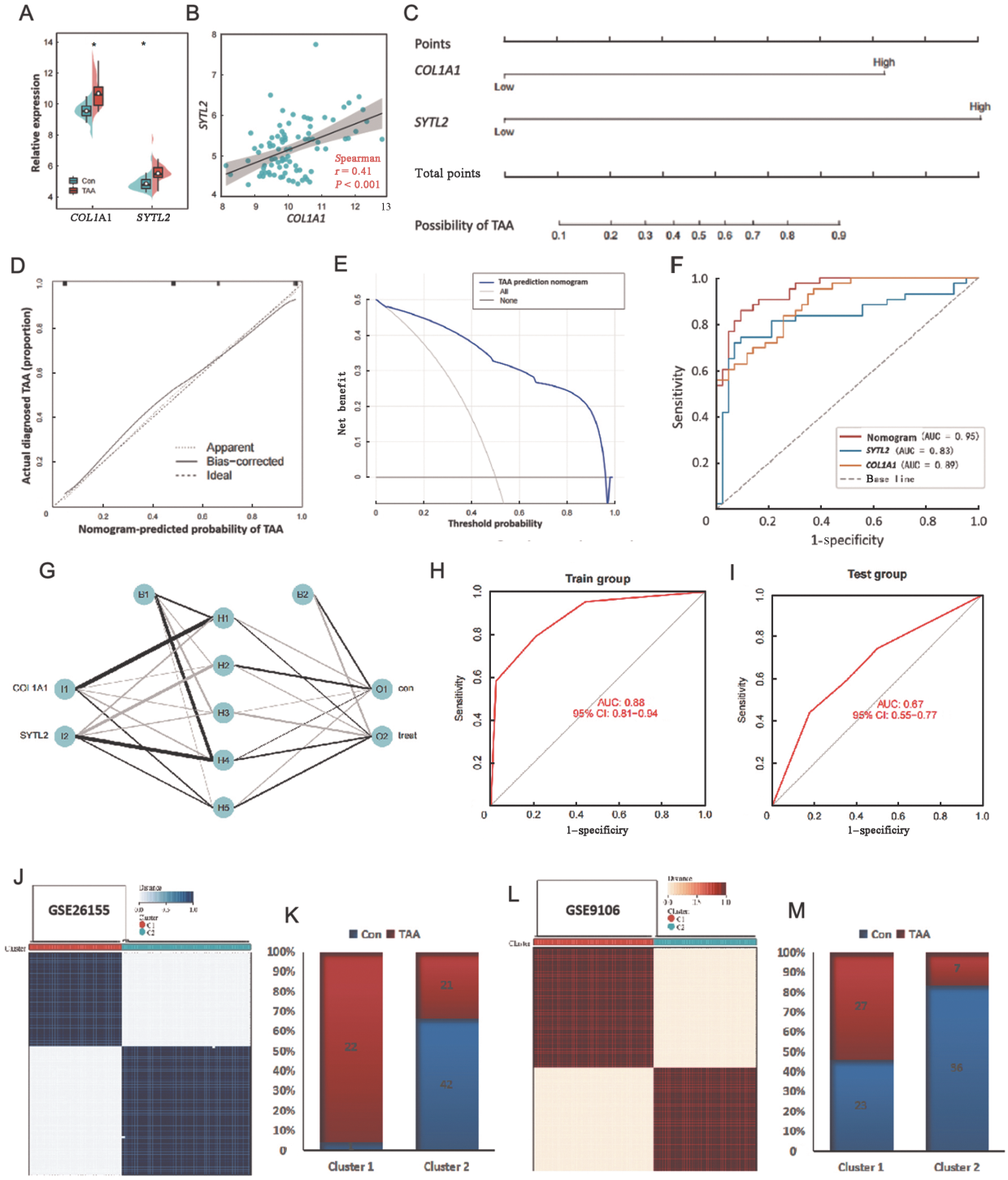

Figure 3: Verification of the diagnostic markers. (A) *COL1A1* and *SYTL2* mRNA expression in TAA compared to normal groups in the vascular wall tissue. (B) The expression levels of *COL1A1* and *SYTL2* showed the positive correlation in the vascular wall tissue. (C) The TAA nomogram was developed with the *COL1A1* and *SYTL2*. (D) Decision curve analysis for the TAA nomogram. (E) Calibration curves of the TAA nomogram prediction. (F) Receiver operating characteristic analysis of the TAA nomogram. (G) The diagnosability of *COL1A1* and *SYTL2* on TAA was tested by a neural network model. (H) ROC curves indicated the diagnosability of the neural network model on the TAA in the GSE26155 set. (I) ROC curves indicated the diagnosability of the neural network model on the TAA in the GSE9106 set. (J,L) Cluster analysis based on *COL1A1* and *SYTL2* in the GSE26155 and GSE9106 datasets, respectively. (K, M) Histogram showed the chi-squared test on the clustering results in the GSE26155 and GSE9106 datasets, respectively. AUC: Area under curve; CI: Confidence interval; Con: Control group; TAA: Thoracic aortic aneurysm; ROC: Receiver operating characteristic.

which showed that the clustering results were similar to the original dataset grouping results [Figure 3K, M].

Immune analysis

These results suggested that inflammatory responses and collagen-related diseases played important roles in TAA pathogenesis. We further explored the function of *COL1A1*, *SYTL2*, and immune cell infiltration in TAA. We compared the immune characteristics of TAA and normal samples by examining the level of immune cell infiltration and immune function using the GSE26155 dataset [Figure 4A]. We analyzed the correlation between TAA and normal groups with immune cell infiltration and immune cell function [Figure 4B, D]. Immune cell infiltration analysis showed that activate dendritic cells (aDCs), B cells, CD8$^+$ T cells, DCs, macrophages, mast cells, neutrophils, plasmacytoid dendritic cells (pDCs), T-helper cells, tumor infiltrating lymphocyte (TIL), and regulatory T cells (Tregs) were higher in patients with TAA than in normal patients [Figure 4C]. Immune cell function analysis showed that APC_co_stimulation, CC chemokine receptor (CCR), checkpoint, cytolytic activity, human leukocyte antigen (HLA), inflammation-promotion, major histocompatibility complex (MHC) class I, para-inflammation, T cell co-inhibition, and type I interferon (IFN) response were more active in patients with TAA than in normal subjects [Figure 4E].

In addition, we analyzed the correlation between the above results of immune infiltration with *COL1A1* and *SYTL2*. *COL1A1* was positively correlated with M2 macrophages but significantly negatively correlated with CD4 naive T cells, Tregs, monocytes, and activated NK cells [Figure 5A]. *SYTL2* was positively correlated with M2 macrophages, CD4 memory resting T cells, M1 macrophages, activated mast cells, and plasma cells, but significantly negatively correlated with CD4 naive T cells, monocytes, M0 macrophages, CD8$^+$ T cells, Tregs, and activated NK cells [Figure 5B].

Single-cell analysis and validation

Together with previous observations that *SYTL2* and *COL1A1* might display diagnostic markers in TAA, we proposed that the upregulation of *SYTL2* and *COL1A1* maybe facilitates the progress of TAA. To further validate our results, we downloaded the GSE155438 dataset for single-cell analyses. Following the quality control standard and normalization of TAA scRNA-seq data, 2980 low-quality cells were excluded, and 1835 cells were included in the analysis [Supplementary Figure 2A, http://links.lww.com/CM9/B669]. The number of genes detected was significantly related to sequencing depth [Supplementary Figure 2B, http://links.lww.com/CM9/B669]. A total of 16,470 corresponding genes were included, and variance analysis revealed 1500 highly variable genes [Supplementary Figure 2C, http://links.lww.com/CM9/B669]. Principal component analysis (PCA) was performed to identify the available dimensions and screen for correlated genes [Supplementary Figure 2D, http://links.lww.com/CM9/B669]. We selected 20 principal components (PCs) with an estimated P value <0.05 for subsequent analysis [Supplementary Figure 2E, http://links.lww.com/CM9/B669].

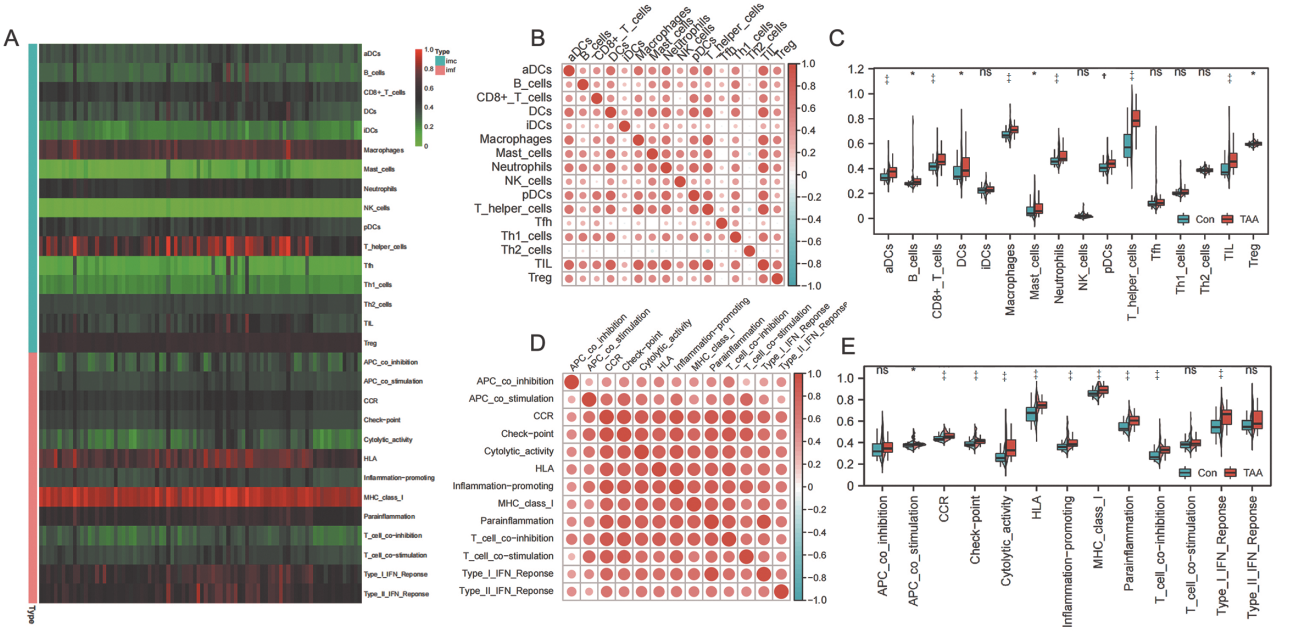

Figure 4: Analysis of immune cell infiltration in aortic wall. (A) The heat map of the immune cells and immune functions in TAA. (B, D) Correlation heat map of immune cells and immune functions. The size of the colored squares represents the strength of the correlation. The redder the color, the stronger the correlation. (C, E) Differential immune cell infiltration and immune functions between the TAA and Con group. $^*P$ <0.05; $^\dagger P$ <0.01; $^\ddagger P$ <0.001. aDCs: Activate Dendritic Cells; iDCs: Immaturate Dendritic Cells; pDCs: Plasmacytoid Dendritic Cells; IFN: Interferon; TAA: Thoracic aortic aneurysm. NK: Natural killer; DC: Dendritic cells; TIL: Tumor infiltrating lymphocyte; Treg: Regulatory cells; Tfh: Follicular helper T cell; CCR: Chemokine receptors; HLA: Human leukocyte antigen; APC: Antigen-presenting cells; MHC: Major histocompatibility complex; TFN: Taxifolin; ns: No significance.

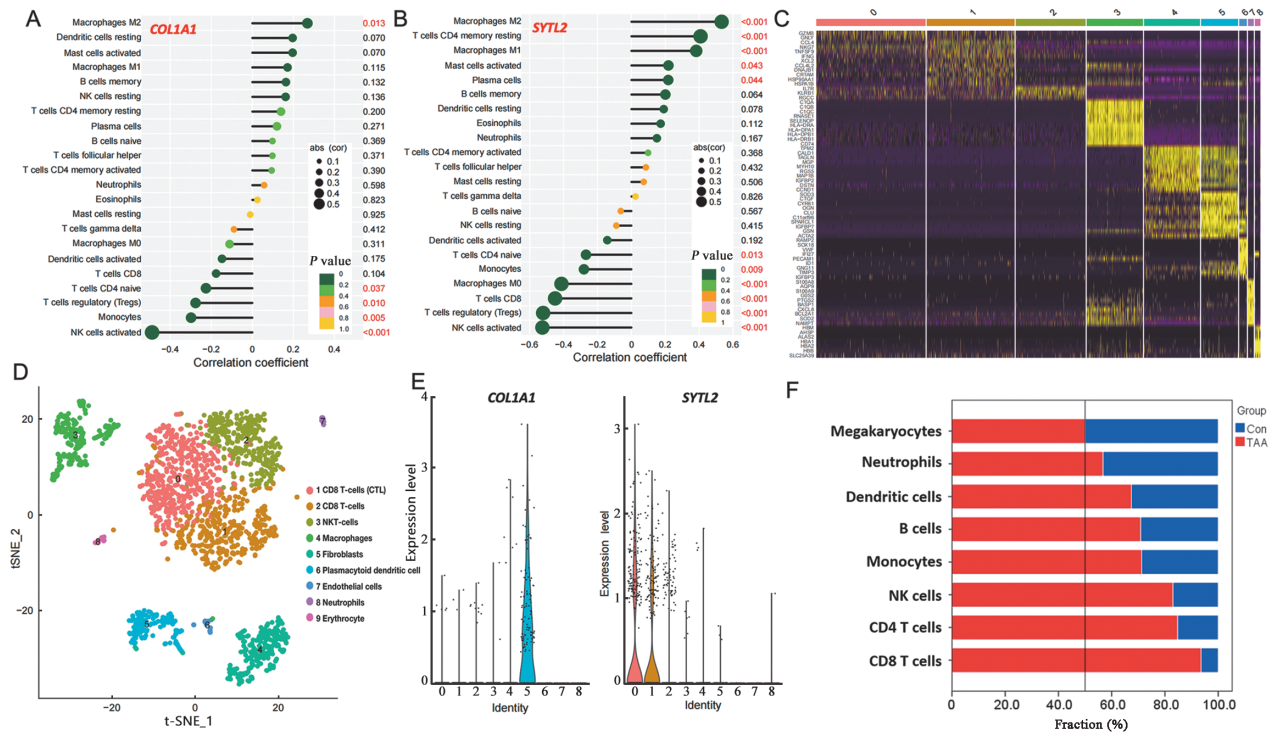

Figure 5: Single cell analysis of aortic wall and infiltrating immune cell component analysis. (A) Correlation between *COL1A1* and infiltrating immune cells and functions in TAA. (B) Correlation between *SYLT2* and infiltrating immune cells and functions in TAA. (C) The differential analysis identified marker genes. The top 20 marker genes of each cell cluster are displayed in the heatmap. A total of 96 genes are listed beside the heatmap after omitting the same top marker genes among clusters. The colors from purple to yellow indicate the gene expression levels from low to high. (D) A t-SNE (annotated by singleR and CellMarker) plot showing all cells of aortas colored according to 9 cell types. (E) Expression levels of *COL1A1* and *SYTL2* in TAA, as well as in other clusters based on scRNA-seq data. (F) The composition of each cell type between TAA and control group was shown in the horizontal bar plot. TAA: Thoracic aortic aneurysm; t-SNE: T-distributed stochastic neighbor embedding. CD: Cluster of differentiation; NK: Natural killer ; Con: Control group; abs: abs function; cor: correlation.Single-cell analysis and validation

The *t*-distributed stochastic neighbor embedding algorithm was applied, and the cells in the human TAA were successfully classified into nine separate clusters. Differential expression analysis was performed, and 5234 marker genes from all nine clusters were identified [Figure 5C]. According to the expression patterns of the marker genes, these clusters were annotated using singleR. Clusters 0, 1, 2, and 8 were annotated as $CD8^+$ T cells, cluster 3 was annotated as macrophages, clusters 4 and 5 were annotated as fibroblasts, cluster 6 as endothelial cells, and cluster 7 as neutrophils [Figure 5D]. In addition, *SYTL2* and *COL1A1* were highly expressed in $CD8^+$ T cell and fibroblast clusters, respectively [Figure 5E]. We examined the source composition of each cell type, we found that the aneurysm tissues contributed more cells than expected in the immune cell group [Figure 5F]. This indicated the gain of more immune cells in the TAA wall, which was consistent with current knowledge. To test our finding, we selected highly expressed genes, *PDGFA*, *PDGFB*, and *CAV1*, as markers for fibroblasts to confirm the observed changes [Figure 6A]. Highly expressed genes, *CD8A, CD8B, and CD28* were selected as markers for $CD8^+$ T cells [Figure 6B].

To determine SYTL2 and COL1A1 expression in the aortas of human TAA, we collected thoracic aorta specimens from six patients with TAA undergoing open aortic repair and aortic specimens from six control subjects who underwent heart transplantation for hypertrophic cardiomyopathy or dilated cardiomyopathy but did not have TAA. Immunofluorescence staining revealed the expression levels of *COL1A1* and *SYTL2* were up-regulated in the artery wall of TAA, and the infiltration level of macrophages was higher than that of the normal control artery wall [Figure 6C, D]. EVG staining revealed the expression levels of collagenous fiber were up-regulated and disordered arrangement in the artery wall of TAA [Figure 6E]. These observations were consistent with the changes we observed in the present study, supporting that the upregulation of *SYTL2* and *COL1A1* might be involved in the inflammatory infiltration of the vessel wall and poor extracellular matrix remodeling, promoting the progression of TAA. The results of this study were summarized briefly, as shown in Figure 7.

Discussion

With aging populations and changes in lifestyles, TAA has become an increasingly important cardiovascular disease.[14] The occurrence of TAA involves multiple factors such as arteriosclerosis, inflammation, immunity, and genetics. The detailed mechanism has not yet been explained, but it has been recognized that the aneurysm formation process is closely related to the destruction of

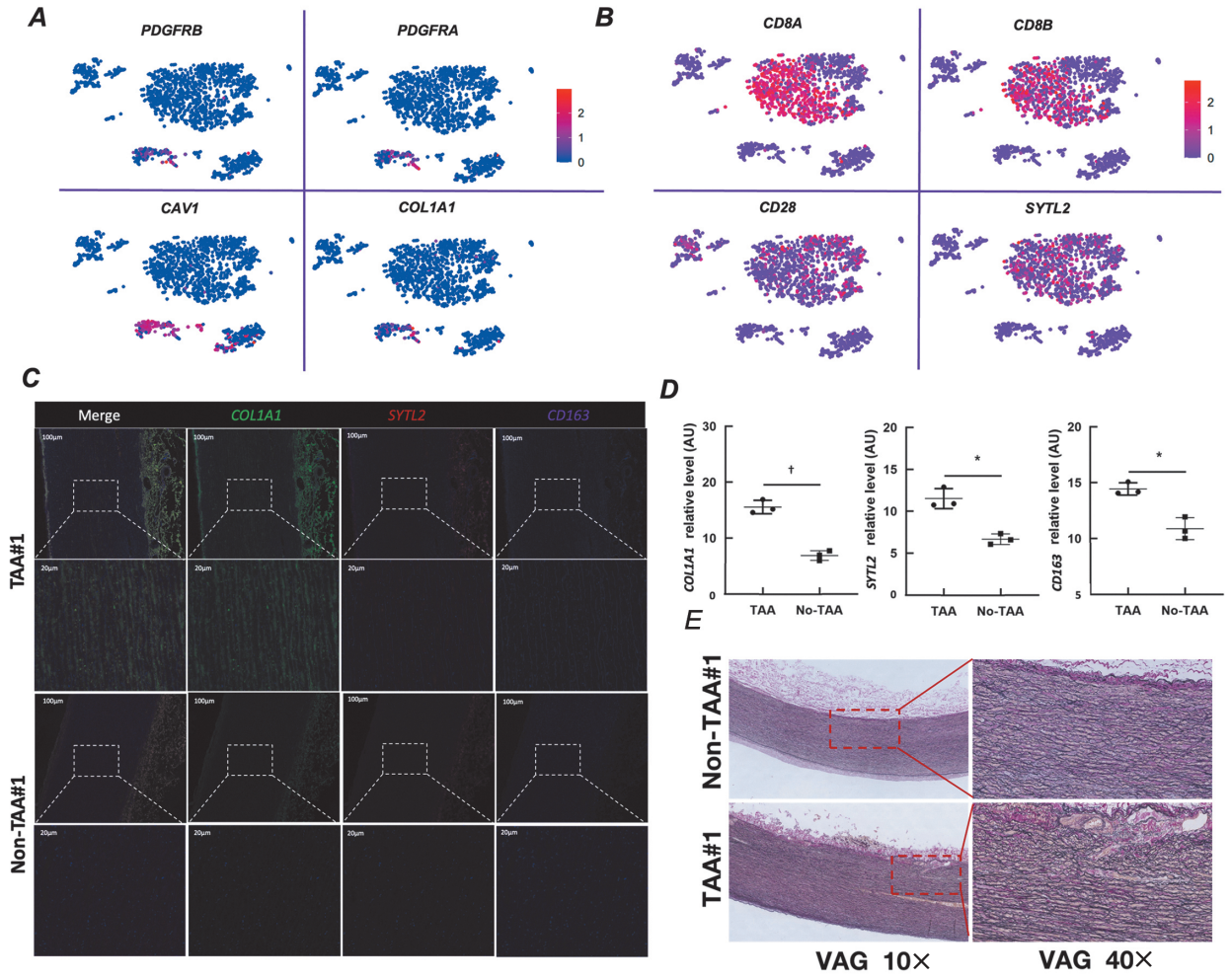

Figure 6: Single-cell analysis of cell populations with high expression of COL1A1 and SYTL2, EVG and multiple immunofluorescence staining verification. (A) Relative expression of *PDGFA, PDGFB, CAV1,* and *COL1A1* in all cells from all samples. Cells were projected onto a t-SNE plot. (B) Relative expression of *CD8A, CD8B, CD28,* and *SYTL2* in all cells from all samples. Cells were projected onto a t-SNE plot. (C) Representative immunofluorescence images and quantification of COL1A1, SYTL2, and CD163 expression. (D) The relative expression level of the COL1A1, SYTL2, and CD163 by the scatter diagram. (E) EVG staining revealed the expression levels of collagenous fiber in the artery wall of TAA. COL1A1: Collagen type I alpha 1 chain; SYTL2: Synaptotagmin like 2; TAA: Thoracic aortic aneurysm; t-SNE: T-distributed stochastic neighbor embedding; EVG: Verhoeff's van gieson; CD163: Cluster of differentiation 163; VAG: Verhoeff's van gieson. $^{*}P<0.05$; $^{\dagger}P<0.01$.

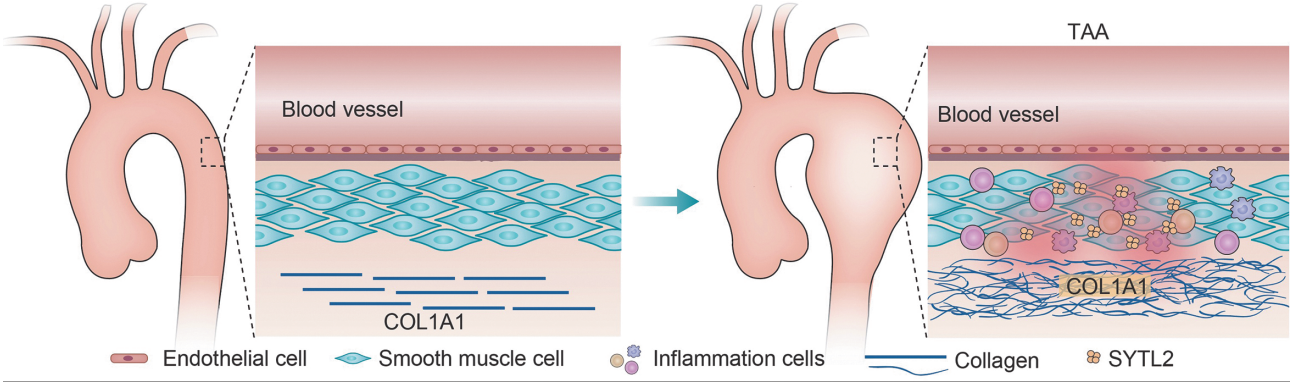

Figure 7: The brief hypothesized mechanism diagram of this study. The expression of SYTL2 in TAA vascular wall tissue and COL1A1 in fibroblasts was significantly higher than that in corresponding normal tissues. The upregulation of SYTL2 and COL1A1 may be involved in the inflammatory infiltration of the vessel wall and poor extracellular matrix remodeling, promoting the progression of TAA. TAA: Thoracic aortic aneurysm. COL1A1: Collagen type I alpha 1 chain; SYTL2: Synaptotagmin like 2.

connective tissue in the arterial wall caused by various factors.[15] By combining the expression profiles of the GSE9106 and GSE26155 datasets, we screened 16 DEGs in TAA compared to normal samples. The enrichment (GO-biological process terms and KEGG pathways) and functional correlation analyses (DO and

GSEA analyses) showed that DEGs were mainly associated with inflammatory response pathways. These results indicated that immune and inflammatory processes characterize the development of TAA, which was consistent with previous findings. Using machine learning algorithms and bioinformatics analysis, we screened the *COL1A1* and *SYTL2* genes to precisely predict TAA. Our results indicated that *COL1A1* and *SYTL2* may serve as biomarkers for TAA and showed a high diagnostic value. Moreover, our study showed that the expression of *COL1A1* and *SYTL2* was significantly upregulated in TAA. Analysis of immune cell infiltration and function showed large immune-inflammatory cell infiltration in TAA, and *COL1A1* and *SYTL2* were significantly correlated with immune cell infiltration and the activation of immune cell functions. Based on the single-cell analysis results, *COL1A1* in TAA was mainly derived from fibroblasts, and *SYTL2* was mainly derived from $CD8^+$ T cells. In addition, single-cell analysis indicated that the number of fibroblasts and $CD8^+$ T cells in TAA was significantly higher than that in normal arterial wall tissue.

Patients with TAA have clear metabolic abnormalities of elastic and collagen fibers, and their histopathological characteristics are elastic fiber sparsity; loss and fracture in the middle membrane to varying degrees; and collagen hyperplasia in the intima, middle membrane, and outer membrane.[16] Changes in collagen expression may be the stress response of the vascular endothelium and vascular SMCs under the action of inflammatory and hemodynamic factors and also one of the reasons for the remodeling of the vascular wall extracellular matrix.[17] Collagens I, III, and V and fibronectin are synthesized by fibroblasts. In addition, fibroblasts secrete MMPs and ECM-degrading enzymes, which play a key role in maintaining extracellular matrix homeostasis.[18,19] The *COL1A1* gene is located on chromosome 17q22 and encodes the front α1 chain of type I collagen fibers.[20] In recent years, it has been reported that there is an abnormal expression of the *COL1A1* gene during tumorigenesis, which may be related to the proliferation and migration of tumor cells and the prognosis of tumors.[21,22] Barzaman *et al*[23] believe that the determination of carbon-terminal fragments of type I collagen fibers in the plasma can be used as a method for predicting bone metastasis of breast cancer. Li *et al*[24] found that COL1A1 can be used as a monitoring factor in early gastric cancer screening to predict poor clinical outcomes in patients. Yang *et al*[25] found that *COL1A1* is highly expressed in gastric cancer tissue and is negatively correlated with the prognosis of patients, involving the extracellular matrix pathway, PI3K-AKT, and other pathways. White *et al*[26] proposed that TAA formation is initiated by the degradation of elastin, during which the intimal elastic fiber product is simultaneously released, which may stimulate an increase in the number of intimal SMCs, which in turn produce MMPs and collagen. Thus, the increase in MMPs and collagen disrupts the homeostasis of elastin and collagen, leading to the expansion of the thoracic aorta to form a TAA.

SYTL2 belongs to the SPFH domain superfamily and is a member of the Stomatin family.[27] SYTL2-hem is carried by exocytic vesicles and participates in cytotoxic granule exocytosis in the lymphocytes.[28] Ménasché *et al*[29] found that SYTL2-hem is carried by exocytic vesicles and participates in cytotoxic granule exocytosis in the lymphocytes. Kesari *et al*[30] suggested that overexpression of recombinant human RAB27A protein (Rab27A)/SYTL2 vesicles in patients with LGMD2B inappropriately signals $CD8^+$ T cell-mediated killing of histocompatibility compatible body (MHC) class I-expressing myofibers. Aberrant release of Rab27A/Slp2a vesicles by myofibers may lead to a pro-inflammatory milieu, culminating in immune cell-mediated myofiber damage. In animal models, AngII promotes vasodilation through the upregulation of AT1R expression in aortic SMCs, and enhanced AngII levels induce vascular SMCs to produce and secrete MCP-1, which then stimulates monocyte recruitment and transformation into macrophages.[31,32] Inflammation of the aorta resulting from the recruitment of inflammatory cells, elevated cytokines, and increased proteolytic enzymes promote medial degeneration and ultimately aneurysm development.[33] Toll-like receptors are classic pattern recognition receptors that play important roles in innate and adaptive immunity. In recent years, an increasing number of scholars have focused on their connection with cardiovascular diseases, such as atherosclerosis, ischemia-reperfusion injury, increased permeability of the vascular wall, and infiltration of inflammatory cells in the vascular wall, leading to arterial tumor occurrence.[34,35]

Although the experimental verification results in this study are consistent with the previous analysis results, the sample size (including single cell sample size) for verification is too small, a larger sample size is needed to further confirm the results of this study. As blood samples were difficult to preserve for a long time, corresponding blood tissue samples were not used for verification in this study, which was also the limitation of our study. The lack of in-depth research and discussion on the pathogenesis of *COL1A1* and *SYTL2* affecting TAA is also the limitation of this study, which needs to be verified and discussed by the later relevant mechanism research.

In conclusion, our results suggest that *COL1A1* and *SYTL2* may be related to TAA, which can be seen as the diagnostic markers with high diagnostic value in the disease. The upregulation of *SYTL2* and *COL1A1* may promote the progression of TAA. Needed more animal experiments and cell experiments to further verify and clarify the mechanism in the future study.

Funding

This work was supported by grants from the National Natural Science Foundation of China (No. 81970412), Xiamen Municipal Health Science and Technology Program Fund (No. 3502Z20194034), Natural Science Foundation of Fujian Province (No. 2022J011414), and Xiamen Medical and Health Guidance Project (No. 3502220214201088).

Conflicts of interest

None.

References

1. Barbour JR, Spinale FG, Ikonomidis JS. Proteinase systems and thoracic aortic aneurysm progression. J Surg Res 2007;139:292–307. doi: 10.1016/j.jss.2006.09.020.
2. Isselbacher EM, Lino Cardenas CL, Lindsay ME. Hereditary influence in thoracic aortic aneurysm and dissection. Circulation 2016;133:2516–2528. doi: 10.1161/circulationaha.116.009762.
3. Joyce JW, Fairbairn JF 2nd, Kincaid OW, Juergen JL. Aneurysms of the thoracic aorta. A clinical study with special reference to prognosis. Circulation 1964;29:176–181. doi: 10.1161/01.cir. 29.2.176.
4. Karthikesalingam A, Bahia S, Patterson BO, Peach G, Vidal-Diez A, Ray KK, *et al*. The shortfall in long-term survival of patients with repaired thoracic or abdominal aortic aneurysms: Retrospective case-control analysis of hospital episode statistics. Eur J Vasc Endovasc Surg 2013;46:533–541. doi: 10.1016/j.ejvs.2013.09.008.
5. Patterson B, Vidal-Diez A, Holt P, Scali S, Beck A, Thompson M. Predicting mid-term all-cause mortality in patients undergoing elective endovascular repair of a descending thoracic aortic aneurysm. Ann Surg 2016;264:1162–1167. doi: 10.1097/sla.0000000000001577.
6. Günay Ş, Güllülü NS. [Approach to aortic aneurysms in the elderly]. Turk Kardiyol Dern Ars 2017;45(Suppl 5):93–95. doi: 10.5543/tkda.2017.57034.
7. Pinard A, Jones GT, Milewicz DM. Genetics of thoracic and abdominal aortic diseases. Circ Res 2019;124:588–606. doi: 10.1161/circresaha.118.312436.
8. Rose NR. Prediction and prevention of autoimmune disease in the 21st century: A review and preview. Am J Epidemiol 2016;183:403–406. doi: 10.1093/aje/kwv292.
9. Lee YH, Petkova AP, Granneman JG. Identification of an adipogenic niche for adipose tissue remodeling and restoration. Cell Metab 2013;18:355–367. doi: 10.1016/j.cmet.2013.08.003.
10. Lee YH, Petkova AP, Konkar AA, Granneman JG. Cellular origins of cold-induced brown adipocytes in adult mice. FASEB J 2015;29:286–299. doi: 10.1096/fj.14-263038.
11. Taketani T, Imai Y, Morota T, Maemura K, Morita H, Hayashi D, *et al*. Altered patterns of gene expression specific to thoracic aortic aneurysms: Microarray analysis of surgically resected specimens. Int Heart J 2005;46:265–277. doi: 10.1536/ihj.46.265.
12. Botta DM Jr. Biomarkers for diagnosis in thoracic aortic disease: PRO. Cardiol Clin 2010;28:207–211. doi: 10.1016/j.ccl.2010.01.009.
13. Xu G, Li K, Zhang N, Zhu B, Feng G. Screening driving transcription factors in the processing of gastric cancer. Gastroenterol Res Pract 2016;2016:8431480. doi: 10.1155/2016/8431480.
14. Senser EM, Misra S, Henkin S. Thoracic aortic aneurysm: A clinical review. Cardiol Clin 2021;39:505–515. doi: 10.1016/j.ccl.2021.06.003.
15. Salameh MJ, Black JH 3rd, Ratchford EV. Thoracic aortic aneurysm. Vasc Med 2018;23:573–578. doi: 10.1177/1358863x18807760.
16. Haas KS, Phillips SJ, Comerota AJ, White JV. The architecture of adventitial elastin in the canine infrarenal aorta. Anat Rec 1991;230:86–96. doi: 10.1002/ar.1092300109.
17. White JV, Haas K, Phillips S, Comerota AJ. Adventitial elastolysis is a primary event in aneurysm formation. J Vasc Surg 1993;17:371–381. doi: 10.1067/mva.1993. 43023.
18. Nissen NI, Karsdal M, Willumsen N. Collagens and cancer associated fibroblasts in the reactive stroma and its relation to cancer biology. J Exp Clin Cancer Res 2019;38:115. doi: 10.1186/s13046-019-1110-6.
19. Shay G, Lynch CC, Fingleton B. Moving targets: Emerging roles for MMPs in cancer progression and metastasis. Matrix Biol 2015;4:200–206. doi: 10.1016/j.matbio.2015.01.019.
20. Büttner C, Skupin A, Rieber EP. Transcriptional activation of the type I collagen genes COL1A1 and COL1A2 in fibroblasts by interleukin-4: Analysis of the functional collagen promoter sequences. J Cell Physiol 2004;198:248–258. doi: 10.1002/jcp.10395.
21. Murabito JM, Rosenberg CL, Finger D, Kreger BE, Levy D, Splansky GL, *et al*. A genome-wide association study of breast and prostate cancer in the NHLBI's Framingham Heart Study. BMC Med Genet 2007;8:S6. doi: 10.1186/1471-2350-8-s1-s6.
22. Turashvili G, Bouchal J, Baumforth K, Wei W, Dziechciarkova M, Ehrmann J, *et al*. Novel markers for differentiation of lobular and ductal invasive breast carcinomas by laser microdissection and microarray analysis. BMC Cancer 2007;7:55. doi: 10.1186/1471-2407-7-55.
23. Barzaman K, Karami J, Zarei Z, Hosseinzadeh A, Kazemi MH, Moradi-Kalbolandi S, *et al*. Breast cancer: Biology, biomarkers, and treatments. Int Immunopharmacol 2020;84:106535. doi: 10.1016/j.intimp.2020.106535.
24. Li J, Ding Y, Li A. Identification of COL1A1 and COL1A2 as candidate prognostic factors in gastric cancer. World J Surg Oncol 2016;14:297. doi: 10.1186/s12957-016-1056-5.
25. Yang W, Pan Y, Guan P, Li X, You C. Bioinformatics analysis of COL1A1 regulated by miR-129-5p as a potential therapeutic target for gastric cancer (in Chinese). J South Med Univ 2019;39:540–546. doi: 10.12122/j.issn.1673-4254.2019.05.07.
26. White JV, Ryjewski C, Trinidad M, Rosenblum J, Platsoucas C. Aortic aneurysm: Search for the trigger. Ann Vasc Surg 2007;21:292–295. doi: 10.1016/j.avsg.2007.03.008.
27. Wang Y, Morrow JS. Identification and characterization of human SLP-2, a novel homologue of stomatin (band 7.2b) present in erythrocytes and other tissues. J Biol Chem 2000;275:8062–8071. doi: 10.1074/jbc.275.11.8062.
28. Christie DA, Kirchhof MG, Vardhana S, Dustin ML, Madrenas J. Mitochondrial and plasma membrane pools of stomatin-like protein 2 coalesce at the immunological synapse during T cell activation. PLoS One 2012;7:e37144. doi: 10.1371/journal.pone.0037144.
29. Ménasché G, Ménager MM, Lefebvre JM, Deutsch E, Athman R, Lambert N, *et al*. A newly identified isoform of Slp2a associates with Rab27a in cytotoxic T cells and participates to cytotoxic granule secretion. Blood 2008;112:5052–5062. doi: 10.1182/blood-2008-02-141069.
30. Kesari A, Fukuda M, Knoblach S, Bashir R, Nader GA, Rao D, *et al*. Dysferlin deficiency shows compensatory induction of Rab27A/Slp2a that may contribute to inflammatory onset. Am J Pathol 2008;173:1476–1487. doi: 10.2353/ajpath.2008.080098.
31. Bani-Sacchi T, Bianchi S, Bani G, Bigazzi M. Ultrastructural studies on white adipocyte differentiation in the mouse mammary gland following estrogen and relaxin. Acta Anat 1987;129:1–9. doi: 10.1159/000146368.
32. Tang W, Zeve D, Suh JM, Bosnakovski D, Kyba M, Hammer RE, *et al*. White fat progenitor cells reside in the adipose vasculature. Science 2008;322:583–586. doi: 10.1126/science.1156232.
33. Emini Veseli B, Perrotta P, De Meyer GRA, Roth L, Van der Donckt C, Martinet W, *et al*. Animal models of atherosclerosis. Eur J Pharmacol 2017;816:3–13. doi: 10.1016/j.ejphar.2017.05.010.
34. Pond CM. Accuracy and artistry in anatomical illustration of perivascular adipose tissue. Front Physiol 2017;8:990. doi: 10.3389/fphys.2017.00990.
35. Tanaka K, Sata M. Roles of perivascular adipose tissue in the pathogenesis of atherosclerosis. Front Physiol 2018;9:3. doi: 10.3389/fphys.2018.00003.

How to cite this article: Xie XS, Yuan Y, Huang YL, Hong X, Hong SC, Chen G, Chen YH, Lin Y, Lu WF, Fu WG, Wang LX. Effects of *COL1A1* and *SYTL2* on inflammatory cell infiltration and poor extracellular matrix remodeling of the vascular wall in thoracic aortic aneurysm. Chin Med J 2024;137:1105–1114. doi: 10.1097/CM9.0000000000002808